

GEOMETRIC ACCURACY OF A STRUCTURED LIGHT SYSTEM

Antonio Maria Garcia Tommaselli

São Paulo State University - Unesp
Campus at Presidente Prudente, S.P.
e_mail: tomaseli@prudente.unesp.br
BRAZIL

Commission II, Working Group 8

KEY WORDS: Reconstruction, Triangulation, Vision, Calibration, Automation, Close_Range Photogrammetry.

ABSTRACT

Geometric accuracy of a structured light system is assessed in this paper considering surface reconstruction as its main purpose. The system is based on off-the-shelf digital camera and a pattern projector. The mathematical model for reconstruction is based on the parametric equation of the projected straight line combined with collinearity equations. The projector calibration is based on the ΔZ method used to determine the perspective centre coordinates in independent model triangulation with analogue photogrammetric stereoplotters. A sequential approach for system calibration was developed and it is presented. Results obtained from real data are also presented and discussed. Experiments with real data using a prototype have indicated 0.5mm of accuracy in height determination and 0.2mm in the XY plane considering an application where the object was 1630mm apart from the camera.

1. INTRODUCTION

In this paper the geometric accuracy of a photogrammetric structured light system is assessed after calibration with real data. This system is currently under development at Unesp-Presidente Prudente, Brazil and a prototype has been available. The project was proposed to meet the requirements of users interested in body surface measurements, aiming scoliosis diagnosis. Previous research projects were conducted using non-metric cameras to measure body surface shapes aiming clinical applications such as diagnosis of postural problems associated with scoliosis, mastectomy and other diseases. The application of conventional analogue or analytical Photogrammetry was unsuitable due to several reasons:

- texture of the human body is homogenous and stereoscopic measurement with floating marks is inaccurate and may produce spurious results;
- there is a need for a high degree of automation, because of non-specialists have to deal with the system routinely and it is desirable that they could perform the measurements;
- the whole conventional photogrammetric systems are quite expensive for these applications;
- real time responses are often required.

Digital Photogrammetry seems to fulfil these needs and high precise close range surface measurements can be achieved. The traditional stereo configuration is avoided in this project due to the problems associated with correspondence determination. An active pattern projector can be introduced and treated as an active camera and only one digital imaging camera may be used. This arrange is similar to triangulation with structured

light (Guisser et al, 1992).

This paper presents the first results with a prototype of a photogrammetric system composed of low cost hardware, based on a pattern projector, a digital camera and software.

2. GEOMETRIC SOLUTION

The proposed approach can be seen as a fusion between an stereo and a structured light system. The projector is treated as a second camera and can be conveniently used as a source of reliable geometric information after a bundle calibration.

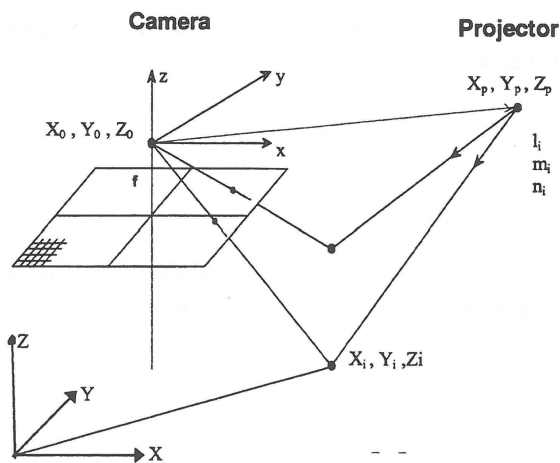


Fig. 1 Geometry of the camera-projector system.

The main contribution of our proposal is to avoid inner calibration of the projector by computing only each straight line equation of the projected bundle instead of inner orientation parameters of the projector. This direct solution eliminates the need for a complex mathematical model and it is also expected that even non parameterised errors in the camera model could be absorbed by the straight line equations.

Figure 1 depicts the geometric concept of the system. The mathematical model is based on the well known collinearity equations. Considering an arbitrary global reference system and the camera reference system, both systems are related through equation (1):

$$\begin{aligned} x_i &= -f \frac{r_{11}(X_i - X_0) + r_{12}(Y_i - Y_0) + r_{13}(Z_i - Z_0)}{r_{31}(X_i - X_0) + r_{32}(Y_i - Y_0) + r_{33}(Z_i - Z_0)} \\ y_i &= -f \frac{r_{21}(X_i - X_0) + r_{22}(Y_i - Y_0) + r_{23}(Z_i - Z_0)}{r_{31}(X_i - X_0) + r_{32}(Y_i - Y_0) + r_{33}(Z_i - Z_0)} \end{aligned} \quad (1)$$

In the collinearity equations (1), (X_i, Y_i, Z_i) are the coordinates of a generic point in the object space, x_i, y_i are the refined image coordinates of the same point, the r_{ij} are the elements of the rotation matrix and f is the camera focal length. The exterior orientation parameters of the camera reference system with respect to the global reference system must be computed, considering an arbitrary sequence of rotations. In this work the adopted rotation matrix, defined by the sequence $M_z(\kappa) M_y(\phi) M_x(\omega)$ is given below (2).

$$\begin{bmatrix} \cos\phi \cdot \cos\kappa & \cos\omega \cdot \sin\kappa + \sin\omega \cdot \sin\phi \cdot \cos\kappa & \sin\omega \cdot \sin\kappa - \cos\omega \cdot \sin\phi \cdot \cos\kappa \\ -\cos\phi \cdot \sin\kappa & \cos\omega \cdot \cos\kappa - \sin\omega \cdot \sin\phi \cdot \sin\kappa & \sin\omega \cdot \cos\kappa + \cos\omega \cdot \sin\phi \cdot \sin\kappa \\ \sin\phi & -\sin\omega \cdot \cos\phi & \cos\omega \cdot \cos\phi \end{bmatrix} \quad (2)$$

The exterior orientation parameters are:

$$[\kappa, \phi, \omega, X_0, Y_0, Z_0]^T \quad (3)$$

An inverse similarity transformation, from image to object space can be defined:

$$\begin{bmatrix} X_i \\ Y_i \\ Z_i \end{bmatrix} = \lambda_i \cdot \begin{bmatrix} r_{11} & r_{12} & r_{13} \\ r_{21} & r_{22} & r_{23} \\ r_{31} & r_{32} & r_{33} \end{bmatrix} \cdot \begin{bmatrix} x_i \\ y_i \\ -f \end{bmatrix} + \begin{bmatrix} X_0 \\ Y_0 \\ Z_0 \end{bmatrix} \quad (4)$$

where λ_i is an unknown that must be computed using both the information from the camera and from the projector.

Regarding to the projector, the parametric equation of a projected straight line is given by:

$$\begin{aligned} X_i^p &= X_p + \lambda_i^p l_i \\ Y_i^p &= Y_p + \lambda_i^p m_i \\ Z_i^p &= Z_p + \lambda_i^p n_i \end{aligned} \quad (5)$$

where:

- (X_p, Y_p, Z_p) are the coordinates of a known point in the projected straight line which is may be perspective centre of the projector;
- (l_i, m_i, n_i) are the direction cosines of each projected ray;
- λ_i^p is a parameter that can be associated to the distance between the projector perspective centre and the generic point in the object space.

In equation (5) the superscript p have been used to denote information acquired from the projector geometry.

Let us rearrange equation (4) using the camera geometric information:

$$\begin{aligned} X_i &= \lambda_i \cdot u_i + X_0 \\ Y_i &= \lambda_i \cdot v_i + Y_0 \\ Z_i &= \lambda_i \cdot w_i + Z_0 \end{aligned} \quad (6)$$

where:

$$\begin{aligned} u_i &= r_{11}x_i + r_{21}y_i + r_{31}(-f) \\ v_i &= r_{12}x_i + r_{22}y_i + r_{32}(-f) \\ w_i &= r_{13}x_i + r_{23}y_i + r_{33}(-f) \end{aligned} \quad (7)$$

Considering that in equations (5) and (6) the coordinates of a generic point are the same in both equations, λ_i^p and λ_i can be determined using equations (8) and (9):

$$\lambda_i = \frac{(X_p - X_0) \cdot n_i - (Z_p - Z_0) \cdot l_i}{n_i \cdot u_i - w_i \cdot l_i} \quad (8)$$

$$\lambda_i^p = \frac{(X_p - X_0) \cdot w_i - (Z_p - Z_0) \cdot u_i}{n_i \cdot u_i - w_i \cdot l_i} \quad (9)$$

These equations are quite similar to those developed for space intersection (See ASP (1980)

Object space coordinates can be obtained by introducing the computed λ_i^p into equation (5). The same approach can be done by using equations (8) and (4). A more reliable estimation can be obtained by using the average value from equations (4) and (5).

3. SYSTEM COMPONENTS

3.1 Digital Camera

Several models of digital cameras have been commercially available recently and most of them can be successfully applied to built digital reconstruction systems. Our prototype has integrated a Kodak DC40, which has a CCD with a resolution of 768x512 pixels (6,9mm x 4,6mm) and progressive scanning. The camera focal length is 46mm equivalent, which means that an theoretic imaging area of 34.5mm x 23mm, with a pixel size of 45 μ m, must be considered. On the other hand, considering the actual CCD imaging area of 6,9mm x 4,6mm and the pixel size of 9 μ m a reduced focal length of 9.2 mm should be used.

Other highest resolution digital cameras probably could give better results, but it seems that this model compares favourably with off-the-shelf video cameras. Nowadays, we are also integrating a Kodak DC 210, with higher resolution, to the prototype. Fig. 2 depicts the Kodak DC40 digital camera.

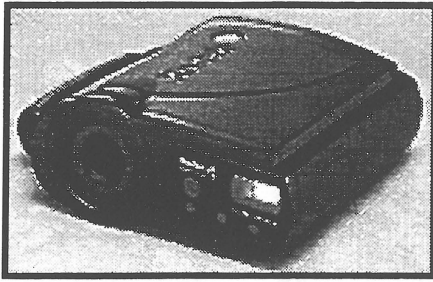


Figure 2 Digital Camera

3.2 Pattern projector

The pattern projector is the second element in the system and it provides both the structured illumination and the geometric information that are used to reconstruct the scene. The structured illumination provides some cues to enhance the correspondence process. Pre-defined targets are easier to locate in the image and can be measured with higher accuracy, for example circular targets. Geometric information is provided by the parameters of the projected ray, which are to be used with camera coordinates to compute object space coordinates, as presented in the previous section.

The pattern projector is an ordinary slide projector, which was reassembled in a mount with a mirror and the digital camera. The mirror can be used to redirect the projected bundle. The pattern was printed using photographic process and inserted within two glasses plates. Figure 3 presents the final configuration of the prototype, integrating the digital camera and the pattern projector.

The whole system configuration includes a calibration plate, which has 20 control points, 6 of which where 200 mm apart from the projection plane. In figure 4 the control and the projected points can be seen. The prototype was attached to the

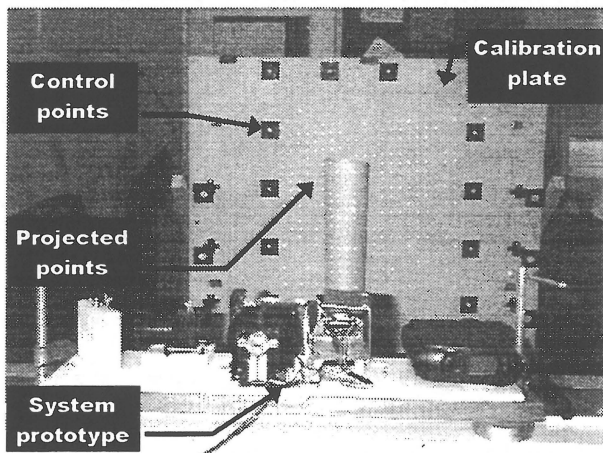


Figure 4 Prototype being used

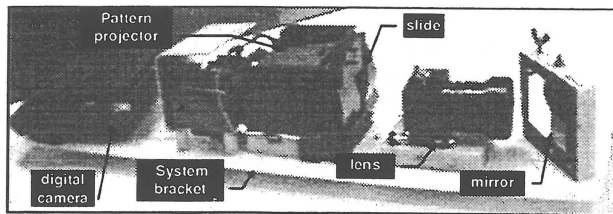


Figure 3 Final configuration of the prototype.

carrier of a rectangular plotter, in order to accurately measure its displacements in the calibration step.

4. FEATURE EXTRACTION

The pattern projected onto the surface must be designed to make feasible image analysis in real time, e.g. a set of cross lines, squares or dots. In order to improve the correspondence process it is recommended to design a pattern with distinct spots, both in shape and dimension. The feature extraction process attempts to detect, recognise and "measure" the projected lines onto the object. Several methods have been implemented from the assisted measurement in the computer screen to the automatic extraction both with least squares matching and with region grouping. Although these methods are high precision, in some cases they could fail in the identification of the targets and could provide wrong correspondences because the pattern has similar targets. This step is still under development and more robust techniques are being studied.

For the case study, the coordinates of the targets where extracted by direct measurement which can ensure the correct identification but the precision is limited to 1 or 1/2 pixel size.

5. SYSTEM CALIBRATION

The system calibration involves the determination of the camera inner orientation parameters and the parametric equations of all projected straight lines. This concept is depicted in figure 5.

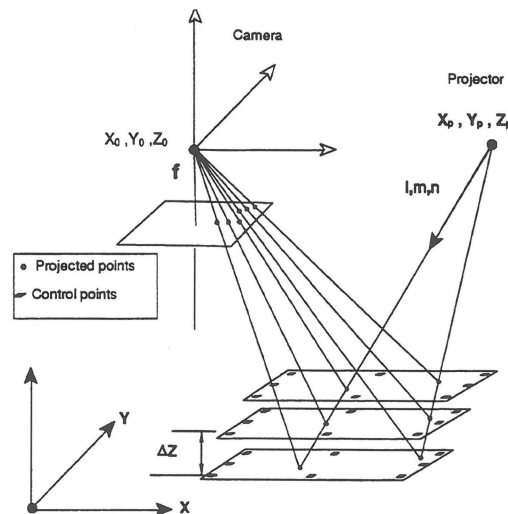


Figure 5 Reference system and the geometric concept of the calibration method.

Although the simultaneous estimation of those parameters would be desirable, experiments have demonstrated unreliable results due to singularities in the normal system equations and high computational costs. Based on this experience, a sequential solution was derived. It involves seven steps, which are summarised in figure 6.

5.1 Camera calibration

The first step in the system calibration is the camera calibration. The camera is calibrated using self calibrating bundle adjustment with convergent cameras. The DC40 has a fixed focus and it is expected that the calibration parameters remains unchanged for a period. A set-up with 48 circular targets was used and convergent images were acquired. The mathematical model for camera calibration is simplified because the CCD has squared pixel and the coverage angle is narrow. Only first order radial lens distortions (k_1), coordinates of the principal point (c_x and c_y) and the focal length (f) have been considered as the camera inner parameters.

5.2 Calibration of the projected bundle

The concept of projector calibration method is similar to the ΔZ method used to determine the perspective centre coordinates in independent model triangulation with analogue photogrammetric stereoplotters. Several images of the projected bundle are acquired on the parallel reference planes which have targets to be used as control points. Different image coordinates of a projected point in several planes will correspond to the same straight line in the object space. Control points will be used to compute the projection plane position and orientation with respect to the camera reference system. Therefore, projected points coordinates over the plane can be computed both in the global and in the camera reference systems.

Camera calibration is the first step and can be performed previously, supposing that the inner orientation elements are stable.

In the second step control points on the calibration plate are identified and measured.

The third step involves the identification and measurement of projected points coordinates for each image collected. Control points and projected points are extracted using methods of feature extraction or by direct measurement the computer screen.

In the fourth step position and orientation parameters of the camera with respect to the control points are computed using Space Resection procedures. Accurate results were only obtained after the introduction of six non coplanar control points, 200mm apart from the calibration plate.

The fifth step attempts to compute the 3D coordinates of the projected points in the global reference system, using the position and orientation parameters previously computed and the image coordinates (measured in step 3). These coordinates are computed using eq. (10).

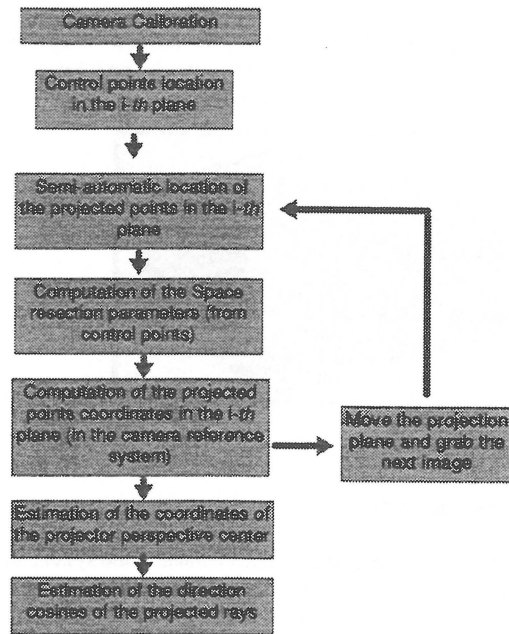


Figure 6 Steps in system calibration

$$\begin{aligned}
 X_i &= X_0 + (Z_i - Z_0) \frac{r_{11} X_i + r_{21} Y_i - r_{31} f}{r_{13} X_i + r_{23} Y_i - r_{33} f} \\
 Y_i &= Y_0 + (Z_i - Z_0) \frac{r_{12} X_i + r_{22} Y_i - r_{32} f}{r_{13} X_i + r_{23} Y_i - r_{33} f} \\
 Z_i &= Z_{\text{plano}}
 \end{aligned} \tag{10}$$

All the Z coordinates of the projected points are considered to be the same, supposing that the plate is a really flat surface. Once the reference plane is moved, another image is grabbed and steps 2, 3, 4 and 5 are repeated, until, at least, information from three planes has been available.

Coordinates of the projector perspective centre are estimated in the sixth step. The mathematical model and procedures for this computation can be found in Moffit & Mikhail (1980). The observation equations are based on the straight line that fits two projected points and the projector perspective centre, as one can see in fig. 5. The straight line equation in 3D space is given by eq. 11.

$$\frac{X_p - X_a}{X_b - X_a} = \frac{Z_p - Z_a}{Z_b - Z_a} \quad \frac{Y_p - Y_a}{Y_b - Y_a} = \frac{Z_p - Z_a}{Z_b - Z_a} \tag{11}$$

After some algebraic manipulations and associating residual errors (v_x and v_y) to the equations, linear observation equations can be obtained, as seen in eq. (12).

$$\begin{aligned}
 v_x - (Z_b - Z_a)X_p - (X_a - X_b)Z_p &= -(X_a Z_b - X_b Z_a) \\
 v_y - (Z_b - Z_a)Y_p - (Y_a - Y_b)Z_p &= -(Y_a Z_b - Y_b Z_a)
 \end{aligned} \tag{12}$$

Once at least two different points on two planes were available it is feasible to compute the projector perspective centre coordinates, using the Least Squares Method.

Direction cosines of the projected rays are estimated in the seventh step. Using the computed coordinates of the projector perspective centre and the coordinates of the projected points both in the global reference system, direction cosines of each projected ray can be computed using eq. (13) and (14).

$$\begin{aligned}\Delta X^i &= X_p^i - X_a^i \\ \Delta Y^i &= Y_p^i - Y_a^i \\ \Delta Z^i &= Z_p^i - Z_a^i\end{aligned}\quad (13)$$

$$\begin{aligned}l^i &= \frac{\Delta X^i}{(\Delta X^i + \Delta Y^i + \Delta Z^i)^2} \\ m^i &= \frac{\Delta Y^i}{(\Delta X^i + \Delta Y^i + \Delta Z^i)^2} \\ n^i &= \frac{\Delta Z^i}{(\Delta X^i + \Delta Y^i + \Delta Z^i)^2}\end{aligned}\quad (14)$$

For each projection plane a set of direction parameters can be computed and the average value will give the best estimate.

6. RESULTS

6.1 Experiments with simulated data

Extensive experiments with simulated data were performed in order to assess the theoretical accuracy of the system and to study variations in the configurations to design a prototype. From these simulations an accuracy of 1mm in depth and 0.3 in XY plane was expected. These preliminary results were reported in Tommaselli et al (1996).

6.2 Experiments with real data

6.2.1 Camera Calibration

The inner orientation parameters of the Kodak DC40 digital camera were obtained using a self-calibrating bundle adjustment, with the nine images taken from a set of 48 circular targets and with the principal point related to the approximated centre of the frame buffer (378, 252) and considering an approximated scale factor of 0.045 (pixel size). The values of the calibrated inner orientation parameters and their standard deviations are presented in table 1. The posteriori standard deviation ($\hat{\sigma}_0$) indicates an observation error ranging $\frac{1}{2}$ pixel. The target coordinates in the image were measured automatically using a gravity centre criteria.

Table 1 Inner parameters of the digital camera DC40 using 48 control points and 9 images.

| Parameters | Estimated Values | Estimated Standard Deviations |
|-----------------------|------------------|-------------------------------|
| c_x (mm) | -0.133 | 0.052 |
| c_y (mm) | 0.208 | 0.068 |
| k_1 | 0.000063 | 0.000001 |
| f (mm) | 46.981 | 0.066 |
| $\hat{\sigma}_0$ (mm) | 0.025 | |

6.1.2 Projector calibration

The proposed method for the system calibration, including camera calibration, has been implemented in C language. The method was tested with real data, which was collected using the prototype. The global coordinates of the 20 control points located over the calibration plate were measured with an accuracy of 0.1 mm. The projector and the digital camera was both turned on and 3 images were collected. The first position of the prototype was 1640mm apart from the calibration plate. Each image was collected and then the plotter carrier was moved by 100mm in order to generate a displacement between the projected planes. A typical image obtained by this process is presented in fig. 7 showing also the 9 projected points, used to calibrate the projector.

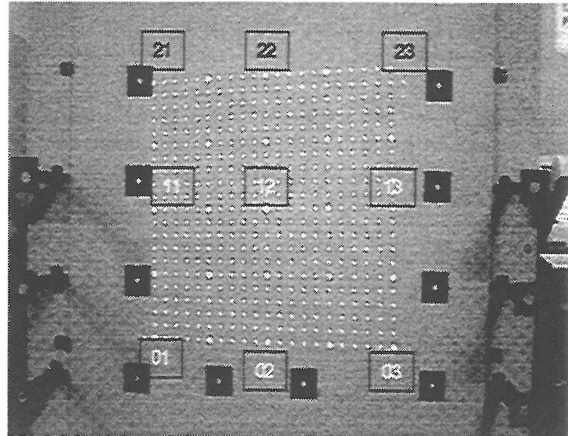


Figure 7 Typical image used in the projector calibration

Table 2 Camera exterior orientation parameters for each projection plane.

| | κ (rad) | ϕ (rad) | ω (rad) | X_0 (mm) | Y_0 (mm) | Z_0 (mm) |
|-----------|----------------|--------------|----------------|------------|------------|------------|
| 1st plane | 0.013301 | 0.01418 | -0.02600 | 375.121 | 364.541 | 1842.675 |
| Dif 2-1 | -0.00008 | -0.00435 | -0.00041 | -5.356 | 1.049 | -101.181 |
| 2nd plane | 0.01321 | 0.00983 | -0.02641 | 369.765 | 365.590 | 1741.494 |
| Dif 3-2 | -0.00047 | 0.00607 | -0.00146 | 12.499 | 3.298 | -102.117 |
| 3th plane | 0.01274 | 0.01590 | -0.02787 | 382.264 | 368.888 | 1639.377 |

The grabbed images had 440 projected points each one (Figure.7) In this experiment only the 16 visible control points and 9 projected points were measured. Visual identification and measurement in the computer screen were used and it is expected that with an automatic measurement process the accuracy of the image coordinates may increase several times. Also, if more projected points were used the whole accuracy of the estimates could be improved. However, even with these conditions the coordinates of the projector perspective centre were accurately estimated, as one can see from the following tables.

In table 2 the camera exterior orientation parameters for each of the three images are presented. The highlighted lines show the differences between these parameters and it can be seen that the angular discrepancies may be neglected while the positional differences are due to the orientation angles of the camera with respect to the global reference system. Residuals in the space resection procedure were within 0,025mm that compares to $\frac{1}{2}$ pixel size.

Table 3 Coordinates of the projector perspective centre

| | X _p (mm) | Y _p (mm) | Z _p (mm) |
|---|---------------------|---------------------|---------------------|
| Coordinates in the camera reference system | -490.304 | 23.837 | 56.8250 |
| Coordinates in the global reference system. | -114.601 | 383.502 | 1905.981 |

Estimated values for the coordinates of the projector perspective centre are presented in Table 3. The second line of this table presents the coordinates in the camera reference system which were obtained applying an inverse similarity transformation to the coordinates in the global reference system using the camera exterior orientation parameters. The original output of the estimation process by ΔZ method were the coordinates in the global reference system which are presented in the third line of table 3.

The direction cosines were estimated using eq. (13) and (14) for each projection plane. The average value considering the three planes for the nine points used in this experiment are presented in table 4.

From these calibrated set (coordinates of the projector perspective centre and direction cosines) and from the image coordinates of a projected point, the 3D coordinates of the surface points can be computed. The 3D coordinates are estimated using the equations presented in section 2.

Table 4 Direction Vectors

| | l _i | m _i | n _i |
|----|----------------|----------------|----------------|
| 01 | 0.09159 | -0.17179 | -0.98087 |
| 02 | 0.24040 | -0.16860 | -0.95592 |
| 03 | 0.38490 | -0.16341 | -0.90838 |
| 11 | 0.09012 | -0.02403 | -0.99564 |
| 12 | 0.23928 | -0.01954 | -0.97075 |
| 13 | 0.38453 | -0.01461 | -0.92300 |
| 21 | 0.08562 | 0.12279 | -0.98873 |
| 22 | 0.23365 | 0.12957 | -0.96365 |
| 23 | 0.37689 | 0.13301 | -0.91666 |

6.2.3 Accuracy of a reconstructed flat surface

In order to evaluate the real accuracy of the proposed approach and the reliability of the prototype an experiment with one of the images of the calibration plane was conducted. The 3D coordinates of the projected points were computed using the calibrated parameters of the projector and the image coordinates of the same points whose direction cosines had been established.

The "reconstructed" coordinates must fit in a plane and its scattering will provide a measure of the system accuracy. The reconstructed coordinates will be compared with the coordinates of the projected points obtained in the fifth step of the calibration process (fig. 6). These projected coordinates were computed using the eq. 10. Table 5 presents the obtained results. The errors with respect to the projection planes are presented in the highlighted lines (Table 5). It is worth of note that there is a systematic effect due to the error in the location of the projector perspective centre. These errors cause a rotation in the reconstructed surface.

Table 5 Reconstructed coordinates and errors with respect to the projected coordinates

| | X (mm) | Y (mm) | Z (mm) |
|----|---------|---------|---------|
| 01 | 43.161 | 85.613 | 216.417 |
| | -1.280 | 0.983 | 16.417 |
| 02 | 310.371 | 83.755 | 216.126 |
| | -3.646 | 1.032 | 16.126 |
| 03 | 602.154 | 76.648 | 214.399 |
| | -5.750 | 0.874 | 14.399 |
| 11 | 38.361 | 341.798 | 216.116 |
| | -1.556 | -1.272 | 16.116 |
| 12 | 302.043 | 348.593 | 215.657 |
| | -3.782 | -1.177 | 15.657 |
| 13 | 589.534 | 355.892 | 215.842 |
| | -5.957 | -1.061 | 15.842 |
| 21 | 31.696 | 592.934 | 216.478 |
| | -1.676 | -3.338 | 16.478 |
| 22 | 295.196 | 610.164 | 215.883 |
| | -3.901 | -3.156 | 15.883 |
| 23 | 581.149 | 628.259 | 213.808 |
| | -5.737 | -2.696 | 13.808 |

A similarity transformation (7 parameters) was then applied the reconstructed coordinates aiming the compensation of the orientation discrepancies between the reconstructed and the real flat surface. The obtained transformation parameters are presented in table 6. The inverse transformation was then applied to the reconstructed points and the errors with respect to the projected points in the global reference system was evaluated.

Table 6 Similarity transformation parameters relating the reconstructed surface and the projected points

| κ | ϕ | ω | X _c | Y _c | Z _c | λ |
|----------|----------|----------|----------------|----------------|----------------|-----------|
| -0.00062 | -0.00299 | 0.00058 | 1.751 | -1.250 | -18.431 | 0.992 |

In Table 7 the reconstructed coordinates after a similarity transformation and the errors with respect to the projected plane are presented. The errors in the reconstructed coordinates are highlighted and show that a high accuracy reconstruction was achieved, even considering the direct measurement of targets and the low resolution of the camera. Although the original reconstructed flat surface were rotated after the transformation, the coordinates scattering with respect to the projection plane was within 0.5 mm. The latest line of table 7 presents the Mean Square Error (MSE) of the errors in the flat surface reconstruction. The MSE for the XY coordinates are around 0.2mm and 0.5mm for Z coordinates. The relative error in Z is 1/3278, considering that the camera is 1639mm apart from the plane surface.

The orientation of the surface was affected mainly by a rotation ϕ around Y axis. This inaccuracy in the surface orientation recovery is greatly influenced by the configuration of the control points which are aligned in Y direction generating a weak geometry to recover the ϕ rotation. The similarity transformation had corrected such a displacement caused by a weak geometry, although the shape of the surface could be considered accurate even in a rotated position.

Table 7 Coordinates of the reconstructed points after a similarity transformation and errors with respect to the projected coordinates

| | X (mm) | Y (mm) | Z (mm) |
|-----|---------|---------|---------|
| 01 | 44.644 | 84.865 | 199.826 |
| | -0.201 | -0.233 | 0.173 |
| 02 | 313.903 | 82.825 | 200.338 |
| | 0.113 | -0.101 | -0.335 |
| 03 | 607.924 | 75.480 | 199.474 |
| | -0.018 | 0.291 | 0.522 |
| 11 | 39.969 | 343.018 | 199.660 |
| | -0.050 | 0.051 | 0.338 |
| 12 | 305.678 | 349.700 | 199.997 |
| | 0.146 | 0.070 | 0.003 |
| 13 | 595.378 | 356.873 | 201.055 |
| | 0.109 | 0.078 | -1.047 |
| 21 | 33.409 | 596.085 | 200.152 |
| | -0.038 | 0.185 | -0.151 |
| 22 | 298.942 | 613.281 | 200.358 |
| | 0.153 | 0.037 | -0.356 |
| 23 | 587.105 | 631.337 | 199.140 |
| | -0.215 | -0.379 | 0.854 |
| MSE | 0.141 | 0.206 | 0.559 |

In order to evaluate the effects of inaccurate camera inner orientation parameters further experiments were performed. Table 8 presents the results of one of these experiments. In this case all the inner parameters were changed to unreal values and the results indicated the degradation in the final accuracy of the reconstructed surface. The MSE of the errors in the coordinates are worse than in the previous experiments and this errors are quite significant. This means, as was expected, that an accurate camera calibration is a key step in the reconstruction process.

Table 8 Results with inaccurate camera inner orientation parameters.

| Camera inner parameters | α_x (mm) | | α_y (mm) | | k_1 | | f (mm) | |
|--|-----------------------|--------------|-----------------------|------------|-----------------------|------------|----------|--|
| | 0.0 | | 0.0 | | 0.0 | | 40.0 | |
| Projection planes | κ (rad) | ϕ (rad) | ω (rad) | X_0 (mm) | Y_0 (mm) | Z_0 (mm) | | |
| | Plane 1 | 0.01298 | 0.02001 | -0.02022 | 379.28 | 361.52 | 1770.43 | |
| σ_x | 0.00153 | 0.01065 | 0.00584 | 19.23 | 10.04 | 2.57 | | |
| Plane 2 | 0.01290 | 0.01631 | -0.02089 | 375.10 | 363.19 | 1676.16 | | |
| σ_x | 0.00174 | 0.01182 | 0.00645 | 20.32 | 10.49 | 2.72 | | |
| Plane 3 | 0.01232 | 0.02347 | -0.02265 | 388.77 | 367.08 | 1581.02 | | |
| σ_x | 0.00190 | 0.01250 | 0.00687 | 20.39 | 10.51 | 2.91 | | |
| MSE of errors in the reconstructed surface | MSE _x (mm) | | MSE _y (mm) | | MSE _z (mm) | | | |
| | 0.702 | | 0.837 | | 0.817 | | | |

The presented results with accurate calibration data enable the assessment of the accuracy of the system. These accuracy, considering the close range environment was within 0.5mm and that is considered suitable for the target application.

The system performance can be improved by:

- Introducing more effective feature extraction methods. Some authors have reported a precision of 0.01 pixel (Trinder et al, 1995) for target measurement;
- Using a high resolution camera, such as a Kodak DCS 420;
- Establishing a more reliable camera calibration setup, with more control points and more images;
- Establishing a different control points configuration, avoiding alignment of the targets;
- Augmenting the number of projected points and projection planes aiming the projector calibration.

7. CONCLUSION

All computer software were written in C language, including image processing routines. The obtained results with the proposed structured light system using real data seems to be suitable to the proposed applications

The results obtained indicated that 0.5mm of accuracy in height determination and 0.2mm in XY plane can be reached, in a typical application. Some questions associated with feature extraction must be further studied aiming the improvement the whole accuracy of the system.

ACKNOWLEDGMENTS

This work was partially supported by CNPq (National Research Council) and FUNDUNESP.

7. REFERENCES

- ASP-American Society of Photogrammetry and Remote Sensing. **Manual of Photogrammetry**. 4th edition, 1980.
- GUISSER, L.; PAYRISSAT, R.; CASTAN, S. A New 3-D Measurement System Using Structured Light, IEEE, 1992.
- MITCHEL, H.L. Applications of digital photogrammetry to medical investigations. **ISPRS Journal of Photogrammetry & Remote Sensing**, Vol. 50, N. 3, 1995.
- MOFFIT, F.H.; MIKHAIL, E.M. **Photogrammetry**. Harper & Row, 1980.
- TOMMASELLI, A.M.G.; SHIMABUKURO, M.H.; SCALCO, P.A.P.; NOGUEIRA, F.M.A. Implementation of a Photogrammetric Range System. In: International Archives of Photogrammetry and Remote Sensing, Viena, 1996.
- TRINDER, J.C.; JANSAN, J.; HUANG, Y. An assessment of the precision and accuracy of methods of digital target location. **ISPRS Journal of Photogrammetry & Remote Sensing**, Vol. 50, N. 2, 1995.